Published in final edited form as:
Cancer Res. 2011 May 1; 71(9): 3182–3188. doi:10.1158/0008-5472.CAN-10-2380.

STAT3 inhibition is a therapeutic strategy for ABC-like diffuse large B cell lymphoma

Anna Scuto[1,*,°], **Maciej Kujawski**[2,°], **Claudia Kowolik**[1], **Ludmila Krymskaya**[3], **Lin Wang**[2], **Lawrence M. Weiss**[4], **David DiGiusto**[3], **Hua Yu**[2], **Stephen Forman**[3], and **Richard Jove**[1]

[1] Molecular Medicine, Beckman Research Institute, City of Hope Comprehensive Cancer Center, Duarte CA

[2] Cancer Immunotherapy and Tumor Immunology, Beckman Research Institute, City of Hope Comprehensive Cancer Center, Duarte CA

[3] Hematology and Hematopoietic Cell Transplantation, Beckman Research Institute, City of Hope Comprehensive Cancer Center, Duarte CA

[4] Pathology, Beckman Research Institute, City of Hope Comprehensive Cancer Center, Duarte CA

Abstract

Persistent STAT3 signaling contributes to malignant progression in many diverse types of human cancer. STAT3 is constitutively active in activated B cell (ABC)-like diffuse large B cell lymphomas (DLBCL), a class of non-germinal center derived DLBCL cells for which existing therapy is weakly effective. In this report, we provide a preclinical proof of concept that STAT3 is an effective molecular target for ABC-like DLBCL therapy. Direct inhibition of STAT3 with shRNA suppressed the growth of human ABC-like DLBCL in mouse models in a manner associated with apoptosis, repression of STAT3 target genes and inhibition of a tumor-promoting microenvironment. Together, these results suggest that STAT3 is essential to maintain the pathophysiology of ABC-like DLBCL and therefore that STAT3 inhibition may offer a promising approach in its therapy.

Keywords

aggressive lymphoma; STAT3; shRNA; STATTIC; mouse models; apoptosis; microenvironment

Introduction

Among the non-Hodgkin's lymphomas, the diffuse large B cell lymphoma (DLBCL) represents the most frequent (30%) of the aggressive lymphomas and is, pathophysiologically and clinically, a very heterogeneous disease(1). In contrast to normal cells, STAT3 is persistently activated in many diverse human tumors, where it dysregulates the transcription of genes involved in fundamental functions such as proliferation, survival, angiogenesis and immune evasion(2).

High levels of STAT3 expression and activation have been found in ABC-like DLBCL(3), which is a subtype of DLBCL associated with a worse prognosis and molecularly

[*]Corresponding Author: Dr. Anna Scuto, Beckman Research Institute, City of Hope Comprehensive Cancer Center, 1500 East Duarte Road, Duarte, CA 91010. Telephone: (626) 256-4673 ext. 64937; Fax: (626) 256-8708; ascuto@coh.org.
[°]Dr. Anna Scuto and Dr. Maciej Kujawski equally contributed to this work

characterized by constitutively activated NF-kB, and differing from GC-like subtype, which is characterized by high levels of CD10 and Bcl-6(4). Recently, it has been demonstrated that Bcl-6 is a negative regulator of STAT3 expression in GC-like DLBCL(3) and also there is cooperation between NF-kB and STAT3 in the ABC-like subtype(5). However, a more detailed study on the role of STAT3 in these tumor cells has not been performed. We analyzed several specimens from ABC-like DLBCL patients by immunofluorescence staining, and in all of them we observed STAT3 activation (Supplemental Figure 1), confirming previous observations(3, 5). We therefore hypothesized that STAT3 inhibition may have anti-lymphoma effects.

The main purpose of this study was to evaluate whether STAT3 could be a good target for treating ABC-like DLBCL. The importance of this study is that treatment with anti-STAT3 drugs directed against this specific target, which is aberrantly activated only in tumors, may be more effective and have fewer side effects than conventional therapy. Our findings demonstrate that inhibition of STAT3 with shRNA suppresses DLBCL tumorigenesis.

Materials and Methods

Establishment of stable transduced cell lines and cell culture conditions

Human ABC-like DLBCL Ly3 and Ly10 cell lines were a gift from Dr. B. Hilda Ye and Dr. L.M. Staudt, respectively. Human GC-like DLBCL DHL-4 cell line was a gift from Dr. M. Jensen. Ly3 and Ly10 cells were maintained in IMDM medium supplemented with 10% FBS and 10% human plasma, respectively. DHL-4 cells were maintained in RPMI medium supplemented with 10% FBS. The lentiviral vectors were produced as described previously(6). Ly3 cells were then transduced at a multiplicity of infection (MOI) of 1. To select the transduced cells the culture medium was replaced after 24 h with fresh medium containing 1 μg/mL puromycin. All the experiments were performed on cells stably transduced with the lentivirus expressing the STAT3 shRNA #842 except those for Figure 2D, where cells were stably transduced with lentivirus expressing STAT3 shRNA #840(6). Mycoplasma testing and Flow Cytometry analysis of a panel of several surface markers expression were done as quality and authenticity control testing of the cell lines studied in this work (data not shown). Tests were performed within the last 6 months.

Drugs and cytokines

STATTIC and S31-201 were provided by EMD Chemicals and were dissolved in 100% DMSO to prepare a 40 mM stock and 25 mM stock, respectively, and stored at −20°C. Recombinant human IL-6 and IL-10 (R&D Systems, Minneapolis, MN) were reconstituted in sterile 1X PBS containing 0.1% BSA to prepare a 10 μg/mL stock and stored at −20°C.

MTS assays

M T S [(3-(4,5-dimethylthiazol-2-yl)-5-(3-carboxymethoxyphenyl)-2-(4-sulfophenyl)-2*H*-tetrazolium, inner salt] assay (Promega, Madison, WI) was performed according to instructions from the supplier. Absorbance was measured at 490 nm with a Chameleon plate reader (Bioscan, Washington DC).

Flow Cytometry

For apoptosis analysis cells were stained with Annexin V and Propidium Iodide (PI) using Annexin V-FITC Apoptosis Detection Kit I (BD Biosciences Pharmingen, San Diego, CA). The percentage of nonviable cells was then determined by flow cytometry. For analysis of phospho-STAT3 levels cells were stained with anti-phospho-STAT3(Y705)-PE (BD Bioscience) or an appropriate isotype control antibody accordingly to published methods(7). At least 50 000 events were collected from each sample using a CyAn ADP Violet (Dako)

cytometer and calculated using the Summit software (Dako) for Figure 1A, while for Figure 4A a Cytomics FC500 (Beckman Coulter) was used and the geometric mean fluorescence intensity was analyzed for live population. The % of dead cells in Figure 1A was calculated considering all the Annexin V-positive plus the PI-positive and the Annexin V/PI-positive cells.

Animal model studies

Ly3 cells (1×10^7) were resuspended in HBSS and injected subcutaneously into the flank of four to six week old athymic nude mice (Taconic Laboratories), NOD/SCID or NOD/SCID IL2Rγ-null mice (Jackson Laboratories, Bar Harbor, ME). All mice were maintained under specific pathogen-free conditions and were used in compliance with protocols approved by the local Institutional Animal Care and Use Committee.

Immunofluorescence staining

Frozen tumor sections were analyzed as described before(8) using primary rabbit anti-cleaved Caspase-3 antibody (1:50, Cell Signaling), followed by secondary antibody (goat anti-rabbit, Alexa Fluor 488 labeled, 1:200, Molecular Probes), and both primary rat anti-mouse Gr1 and CD31 antibodies (1:20, BD Biosciences), followed by secondary goat anti-rat antibody conjugated with Alexa Fluor 555 (1:200, Invitrogen).

Western blot analysis

Tumor samples were homogenized in RIPA lysis buffer, which includedprotease and phosphatase inhibitors. Western blot analysis was performed as described before(9) using the indicated antibody: rabbit polyclonal anti-STAT3 and anti-phospho-STAT3 (Tyr705) (Cell Signaling Technology, Danvers, MA); mouse monoclonal anti-c-Myc and rabbit polyclonal anti-Mcl-1 (Santa Cruz Biotechnology, Santa Cruz, CA); rabbit polyclonal anti-Survivin (Novus Biologicals, Littketon, CO); mouse monoclonal β-actin antibody (Sigma-Aldrich, St Louis, MO).

Cytokine antibody array

Tumor samples were digested in HBSS containing DNAse and collagenase and processed in the strainer. Single-cell suspensions were then cultured in medium for 24 hours. Following that, supernatants were analyzed using human cytokine antibody array (Raybiotech, Norcross, GA) according to the manufacturer's protocol.

Quantitative real-time PCR and PCR arrays

Total RNA was isolated and purified from cells by RNeasy Kit (Qiagen) and reverse-transcribed using the Omniscript Reverse Transcription Kit (Qiagen). For Figure 1C, cDNAs were analyzed by quantitative real-time PCR using primers provided by SABiosciences (Frederick, MD) and iQ SYBR Green supermix (Bio-Rad). For Figure 3C, cDNAs were analyzed using a PCR array system (SABiosciences) according to the manufacturer's protocol. PCRs were carried out on a DNA Engine thermal cycler equipped with Chromo4 detector (Bio-Rad).

Statistical analysis

Statistical analyses were performed using the statistical software GraphPad Prism 4. Statistical significance was set at a level of $P<0.05$.

Results and Discussion

We investigated the effect of STAT3 silencing in three different animal models of Ly3 lymphoma (Nude, NOD-SCID and NOD-SCID IL-2Rnull mice). For this purpose, we established stably transduced STAT3 shRNA-expressing lentivirus Ly3 cells and control lentivirus Ly3 cells. The stable expression of STAT3 shRNA resulted in 40–50% reduction of total STAT3 protein levels compared to the control lentivirus cells (Supplemental Figure 2A).

In vitro experiments revealed that STAT3 down-regulation was associated with a higher percentage of dead cells in STAT3 shRNA cells compared with the control cells, and this percentage was even higher in serum starvation conditions and after 72 h of culture compared to 48 h, suggesting a role for STAT3 in the survival of those cells (Figure 1A). STAT3 silencing inhibited the growth of Ly3 cells (approximately 40% inhibition) even in the presence of IL-6 or IL-10, which are major activators of STAT3 signaling and are important in the pathophysiology of DLBCL(10) (Figure 1B). The percentages of Ly3 cells proliferation at 48 h were comparable to those at 72 h (Supplemental Figure 2B). Similar results were obtained in Ly10 cells, demonstrating that this strategy also affected another ABC-like cell line (Figure 1B). Quantitative real-time PCR revealed that silencing of STAT3 resulted in down-regulation of different STAT3 target genes in a cell-dependent manner. In particular, we observed significant reduction in mRNA levels of Mcl-1, Bcl-xL and Survivin in STAT3 shRNA lentivirus Ly3 cells, as well as significant reduction of Cyclin D2 and up-regulation of STAT1 in STAT3 shRNA lentivirus Ly10 cells (Figure 1C). STAT3 inhibition also reduced adhesion of Ly3 cells to the bone marrow stroma layer and migration toward SDF-1 alpha (data not shown), an important factor that mediates proliferation, survival, chemotaxis, migration and adhesion into bone marrow stroma, and has been shown to be a chemoattractant factor for B-lymphoma cells(11). We extended this strategy to a cell line representing the GC subtype, DHL-4, which shows very low or undetectable levels of phospho-STAT3 by Western or Flow Cytometry analysis (Data not shown). Cell growth and STAT3 target gene expression were not affected in these cells cultured *in vitro* (Data not shown), demonstrating that GC-like DHL-4 cells do not depend on STAT3 in terms of proliferation. These data are in agreement with a previous study, which demonstrated that STAT3 is downregulated in GC-like cells(3). Thus, based on our observations we raise the possibility that GC-like cells may generally not be dependent on STAT3; however, this suggestion needs to be validated with additional GC-like cells.

Tumors in control lentivirus Ly3-bearing mice grew progressively (Figure 2A), whereas tumors in STAT3 shRNA lentivirus Ly3-bearing mice regressed 4–5 days after injection (Figure 2B–C). These results were comparable to those obtained with Ly3 stably transduced with lentivirus expressing a STAT3 shRNA with different sequence than the original one (Figure 2D). Similar results were observed in Ly10 xenografts (Supplemental Figure 3). STAT3 shRNA Ly3 tumor regression was associated with Caspase-3-dependent apoptosis and significant reduction of STAT3 target genes at the protein level such as Mcl-1, c-Myc and Survivin (approximately 40% to 60% inhibition) (Figure 3A). Survivin expression is an unfavorable prognostic factor in DLBCL(12). We also observed 30% reduction of IL-10 production and the secretion of many other cytokines was altered as well (Figure 3B). c-Myc rearrangements and elevated IL-10 plasma levels are associated with poor prognosis in DLBCL(13, 14). While both STAT3 shRNA and control lentivirus Ly3 cells grown *in vitro* had the same protein levels of c-Myc, STAT3 silencing resulted in inhibition of IL-10-inducible upregulation of c-Myc (Supplemental Figure 2C) associated with downregulation of IL-10-dependent STAT3 activation (data not shown) and inhibition of IL-10-inducible cell growth (Figure 1B, left panel and Supplemental Figure 2B). These data suggest a role of IL-10/STAT3/cMyc in Ly3 cell proliferation and reveal a difference between *in vitro* and *in*

vivo, where IL-10 was observed among the cytokines that were produced the most in control tumors and reduced in STAT3 shRNA lentivirus tumors.

It is notable that partial STAT3 down-regulation (40% inhibition of total STAT3 levels were observed by Western blot analysis) results in such dramatic antitumor effects *in vivo.* This implies that Ly3 cells depend strongly on STAT3 for proliferation and survival *in vivo*. While *in vitro* studies did show Ly3 dependency on STAT3 for proliferation and survival, these effects were not as dramatic as the *in vivo* results, suggesting that the tumor microenvironment has a critical role in STAT3-dependent tumor cells. STAT3 signaling is important in crosstalk between tumor cells and stroma cells(15), and through control of expression of multiple factors is involved in induction of angiogenesis and immune evasion(16). Blocking STAT3 in Ly3 cells affected secretion and expression of several factors responsible for migration of diverse stroma cells and pro-tumor microenvironment remodeling (Figure 3B and 3C). The most striking observation is the requirement of STAT3 signaling in lymphoma cells for induction of tumor angiogenesis, as shown by significant reduction of $CD31^+$ endothelial cells infiltration (Figure 3D). Moreover, blocking STAT3 signaling affected infiltration of $Gr1^+$ cells, a sub-population of myeloid cells previously associated with tumor immune suppression and angiogenesis(8, 17). Pro-angiogenic gene signatures of large-B-cell lymphoma were previously associated with poor prognosis(18). Furthermore, blocking STAT3 signaling in Ly3 cells induces expression of genes involved in T cells migration, such as CXCL10, which was shown to be upregulated after blocking of STAT3 in a mouse melanoma model, resulting in increased infiltration of T cells(19).

Finally, we investigated whether small-molecule STAT3 inhibitors had anti-lymphoma activity like the shRNA. We tested two commercially available inhibitors, STATTIC and S31–201. The viability of Ly3 cells grown *in vitro* was affected by both inhibitors tested in a dose-dependent manner and the anti-proliferative effect was associated with inhibition of STAT3 phosphorylation (Figure 4A). The anti-lymphoma activity of STATTIC was also observed in a Ly3 NOD-SCID IL2Rnull mouse model (Figure 4B). The inhibition of tumor growth was significant, but not as dramatic as that mediated by shRNA, most probably due to low efficiency of intratumoral drug bioavailability. Nevertheless, the tumor growth inhibition was associated with decreased levels of phospho-STAT3 in all tumor samples isolated from STATTIC treated mice compared to vehicle treated mice.

Previous reports with STAT3 siRNA or kinase inhibitors such as JAK inhibitors in these tumor cells were limited to proliferation analysis *in vitro*(5, 20). This is the first demonstration *in vivo* that direct STAT3 inhibition in ABC-like DLBCL suppresses tumor growth. Our data also suggest that direct inhibition of STAT3, rather than indirect inhibition targeting upstream signaling, may be more effective as a therapeutic strategy for these tumor types. Moreover, partial inhibition of target genes would be the most likely response in the treatment of patients, due to limited delivery efficiency of the siRNA into tumors. Thus, our results show that even partial down-regulation of STAT3 could achieve complete suppression of the tumorigenesis of ABC-like DLBCL Ly3 cells.

While developing a small-molecule STAT3 inhibitor as well as siRNA delivery for clinical trials is still a challenge, our *in vitro* and *in vivo* studies demonstrate that STAT3 is a good target for therapy in DLBCL and also establish that STAT3 siRNA-based gene therapy is a feasible approach for DLBCL. Our data encourage continued development of new STAT3 inhibitors as well as STAT3 siRNA delivery strategies for treatment of DLBCL.

Supplementary Material

Refer to Web version on PubMed Central for supplementary material.

Acknowledgments

This work was supported by a grant from the National Institute of Health (R01 CA-055652) to R.J., W. M. Keck Foundation and Tim Nesvig Lymphoma Fellowships to A.S.. We thank members of our laboratories for stimulating discussion.

References

1. Swerdlow SH, Campo E, Harris NL, Jaffe ES, Pileri SA, Stein H, et al. WHO Classification of Tumours of Haematopoietic and Lymphoid Tissues. IARC Meeting. 2008
2. Yu H, Jove R. The STATs of cancer--new molecular targets come of age. Nature Reviews. 2004; 4:97–105.
3. Ding BB, Yu JJ, Yu RY, Mendez LM, Shaknovich R, Zhang Y, et al. Constitutively activated STAT3 promotes cell proliferation and survival in the activated B-cell subtype of diffuse large B-cell lymphomas. Blood. 2008; 111:1515–23. [PubMed: 17951530]
4. Lenz G, Staudt LM. Aggressive lymphomas. The New England Journal of Medicine. 362:1417–29. [PubMed: 20393178]
5. Lam LT, Wright G, Davis RE, Lenz G, Farinha P, Dang L, et al. Cooperative signaling through the signal transducer and activator of transcription 3 and nuclear factor-{kappa}B pathways in subtypes of diffuse large B-cell lymphoma. Blood. 2008; 111:3701–13. [PubMed: 18160665]
6. Hedvat M, Huszar D, Herrmann A, Gozgit JM, Schroeder A, Sheehy A, et al. The JAK2 inhibitor AZD1480 potently blocks Stat3 signaling and oncogenesis in solid tumors. Cancer Cell. 2009; 16:487–97. [PubMed: 19962667]
7. Perez OD, Nolan GP. Simultaneous measurement of multiple active kinase states using polychromatic flow cytometry. Nature Biotechnology. 2002; 20:155–62.
8. Kujawski M, Kortylewski M, Lee H, Herrmann A, Kay H, Yu H. Stat3 mediates myeloid cell-dependent tumor angiogenesis in mice. The Journal of Clinical Investigation. 2008; 118:3367–77. [PubMed: 18776941]
9. Scuto A, Kirschbaum M, Kowolik C, Kretzner L, Juhasz A, Atadja P, et al. The novel histone deacetylase inhibitor, LBH589, induces expression of DNA damage response genes and apoptosis in Ph- acute lymphoblastic leukemia cells. Blood. 2008; 111:5093–100. [PubMed: 18349321]
10. Nacinovic-Duletic A, Stifter S, Dvornik S, Skunca Z, Jonjic N. Correlation of serum IL-6, IL-8 and IL-10 levels with clinicopathological features and prognosis in patients with diffuse large B-cell lymphoma. International Journal of Laboratory Hematology. 2008; 30:230–9. [PubMed: 18479302]
11. Arai J, Yasukawa M, Yakushijin Y, Miyazaki T, Fujita S. Stromal cells in lymph nodes attract B-lymphoma cells via production of stromal cell-derived factor-1. Eur J Haematol. 2000; 64:323–32. [PubMed: 10863978]
12. Adida C, Haioun C, Gaulard P, Lepage E, Morel P, Briere J, et al. Prognostic significance of survivin expression in diffuse large B-cell lymphomas. Blood. 2000; 96:1921–5. [PubMed: 10961895]
13. Savage KJ, Johnson NA, Ben-Neriah S, Connors JM, Sehn LH, Farinha P, et al. MYC gene rearrangements are associated with a poor prognosis in diffuse large B-cell lymphoma patients treated with R-CHOP chemotherapy. Blood. 2009; 114:3533–7. [PubMed: 19704118]
14. Lech-Maranda E, Bienvenu J, Michallet AS, Houot R, Robak T, Coiffier B, et al. Elevated IL-10 plasma levels correlate with poor prognosis in diffuse large B-cell lymphoma. European Cytokine Network. 2006; 17:60–6. [PubMed: 16613764]
15. Yu H, Kortylewski M, Pardoll D. Crosstalk between cancer and immune cells: role of STAT3 in the tumour microenvironment. Nat Rev Immunol. 2007; 7:41–51. [PubMed: 17186030]
16. Yu H, Pardoll D, Jove R. STATs in cancer inflammation and immunity: a leading role for STAT3. Nat Rev Cancer. 2009; 9:798–809. [PubMed: 19851315]
17. Kortylewski M, Kujawski M, Wang T, Wei S, Zhang S, Pilon-Thomas S, et al. Inhibiting Stat3 signaling in the hematopoietic system elicits multicomponent antitumor immunity. Nat Med. 2005; 11:1314–21. [PubMed: 16288283]

18. Lenz G, Wright G, Dave SS, Xiao W, Powell J, Zhao H, et al. Stromal gene signatures in large-B-cell lymphomas. N Engl J Med. 2008; 359:2313–23. [PubMed: 19038878]

19. Wang T, Niu G, Kortylewski M, Burdelya L, Shain K, Zhang S, et al. Regulation of the innate and adaptive immune responses by Stat-3 signaling in tumor cells. Nat Med. 2004; 10:48–54. [PubMed: 14702634]

20. Yang C, Lu P, Lee FY, Chadburn A, Barrientos JC, Leonard JP, et al. Tyrosine kinase inhibition in diffuse large B-cell lymphoma: molecular basis for antitumor activity and drug resistance of dasatinib. Leukemia. 2008; 22:1755–66. [PubMed: 18596745]

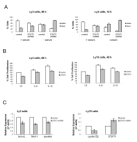

Figure 1. Effects of shRNA-mediated STAT3 inhibition *in vitro*

(A) Control or STAT3 shRNA lentivirus Ly3 cells were grown for 48/72 hours in full or serum free medium. The percentage of viable and dead apoptotic cells was determined by flow cytometry using Annexin V/Propidium Iodide staining. Values represented as bar graphs are the mean of 3 independent experiments with the standard deviation. **(B)** Control or STAT3 shRNA lentivirus Ly3 and Ly10 cells were plated in the presence of medium containing 10% FBS in 96-well plates and incubated with 4 ng/mL IL-6 or IL-10 for 48 hours. Following this, the percentage of cell proliferation was determined by MTS assay. Values represented as bar graphs are the mean of 3 independent experiments with the standard deviation. **(C)** After 48 h of culture cells were collected to isolate RNA and real-time PCR was performed to see changes in mRNA levels of STAT3 target genes. Bars represent relative expression values normalized to the beta-actin levels. Values represented as bar graphs are the mean of 3 independent experiments with the standard deviation.

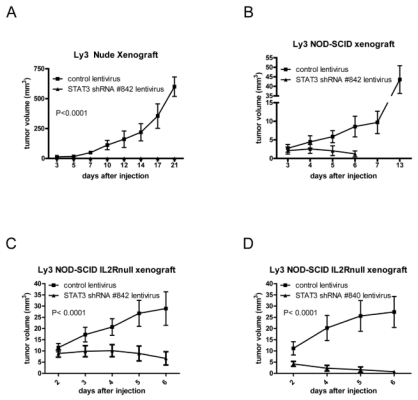

Figure 2. STAT3 silencing inhibits the tumor growth of human ABC-like DLBCL Ly3 cells xenografts

(A) Nude mice (6 mice/group) were injected subcutaneously 24 hours post total body irradiation (3 Gy) (S.C.) with control lentivirus Ly3 cells or STAT3 shRNA lentivirus Ly3 cells. Statistical analysis was performed with Two-way ANOVA. **(B)** NOD-SCID mice (6 mice/group) were injected S.C. with control lentivirus Ly3 cells or STAT3 shRNA lentivirus Ly3 cells. **(C)** NOD-SCID IL2Rnull mice (6 mice/group) were injected S.C. with control lentivirus Ly3 cells or STAT3 shRNA lentivirus Ly3 cells. Statistical analysis was performed with Two-way ANOVA. **(D)** NOD-SCID IL2Rnull mice (6 mice/group) were injected S.C. with control lentivirus Ly3 cells or STAT3 shRNA #840 lentivirus Ly3 cells. Statistical analysis was performed with Two-way ANOVA.

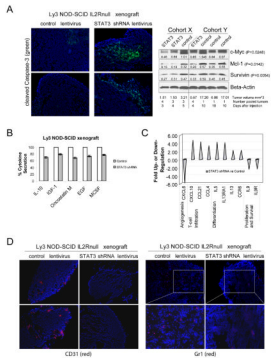

Figure 3. STAT3 silencing induces tumor apoptosis and affects infiltration of tumor microenvironment cells in Ly3 xenografts

(A, left panel) Tumors from control lentivirus or STAT3 shRNA lentivirus NOD-SCID IL2Rnull mice were harvested 6 days post injection, stained with cleaved Caspase-3 antibody and analyzed by immunofluorescence. Nuclei were stained with Hoechst. **(A, right panel)** Two separate cohorts of nude mice were injected S.C. with control lentivirus Ly3 cells or STAT3 shRNA lentivirus Ly3 cells. Tumor samples from each group were harvested at the indicated time and when the volume reached the indicated value; whole-cell lysates were prepared and subjected to Western blotting individually or pooled with tumors harvested from the same group in the same time. Beta-Actin levels served as loading controls. The Integrated Density Values (IDVs) were determined by the densitometry software AlphaImager. Values below each band indicate the ratio between the IDV of that band with the IDV of the correspondent Beta-Actin band. The statistical significance was calculated using the normalized IDVs and the statistical analysis was performed with a student's-t test (unpaired t test with Welch's correction). **(B)** Six days post injection tumors from control lentivirus or STAT3 shRNA lentivirus NOD-SCID mice were isolated, pooled, and processed to perform a cytokine array. Signals were quantified by densitometry and normalized to positive controls. The percentage of cytokine secretion in STAT3 shRNA lentivirus is relative to 100% control lentivirus. **(C)** After 48 h of culture cells were collected to isolate RNA and PCR array was performed to see changes in mRNA levels of inflammatory cytokines and receptors genes. **(D)** Tumors from control lentivirus or STAT3 shRNA lentivirus NOD-SCID IL2Rnull mice were harvested 6 days post injection, stained with CD31 **(left panel)** or Gr1 **(right panel)** antibody and analyzed by immunofluorescence. Nuclei were stained with Hoechst.

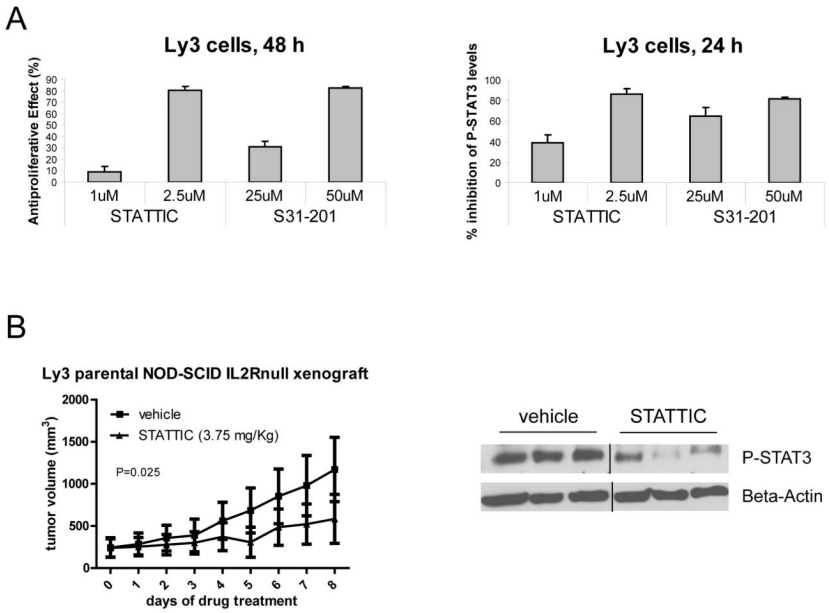

Figure 4. Small-molecule STAT3 inhibitors affect the growth of Ly3 cells *in vitro* and *in vivo*

(A) Ly3 parental cells were plated in the presence of medium containing 10% FBS and treated with STAT3 inhibitors at the indicated concentrations. After 24 or 48 h, phospho-STAT3 level or cell proliferation were analyzed by flow cytometry or MTS assay, respectively. Values represented as bar graphs are the mean of 3 independent experiments with the standard deviation. **(B)** Ly3 parental tumor-bearing mice were treated intra tumor with vehicle or STATTIC at 3.75 mg/kg every day. Two hours after the last treatment, samples from each group were harvested. Whole-cell lysates were prepared and subjected to Western blot analysis for phospho-STAT3 level detection. Beta-Actin levels served as loading controls.